



HAL
open science

Predictions of the arrival time of Coronal Mass Ejections at 1AU: an analysis of the causes of errors

M. Owens, P. Cargill

► **To cite this version:**

M. Owens, P. Cargill. Predictions of the arrival time of Coronal Mass Ejections at 1AU: an analysis of the causes of errors. *Annales Geophysicae*, 2004, 22 (2), pp.661-671. hal-00317248

HAL Id: hal-00317248

<https://hal.science/hal-00317248>

Submitted on 18 Jun 2008

HAL is a multi-disciplinary open access archive for the deposit and dissemination of scientific research documents, whether they are published or not. The documents may come from teaching and research institutions in France or abroad, or from public or private research centers.

L'archive ouverte pluridisciplinaire **HAL**, est destinée au dépôt et à la diffusion de documents scientifiques de niveau recherche, publiés ou non, émanant des établissements d'enseignement et de recherche français ou étrangers, des laboratoires publics ou privés.

Predictions of the arrival time of Coronal Mass Ejections at 1 AU: an analysis of the causes of errors

M. Owens and P. Cargill

Space and Atmospheric Physics, The Blackett Laboratory, Imperial College, London SW7 2BW, UK

Received: 21 March 2003 – Revised: 7 July 2003 – Accepted: 11 July 2003 – Published: 1 January 2004

Abstract. Three existing models of Interplanetary Coronal Mass Ejection (ICME) transit between the Sun and the Earth are compared to coronagraph and in situ observations: all three models are found to perform with a similar level of accuracy (i.e. an average error between observed and predicted 1 AU transit times of approximately 11 h). To improve long-term space weather prediction, factors influencing CME transit are investigated. Both the removal of the plane of sky projection (as suffered by coronagraph derived speeds of Earth directed CMEs) and the use of observed values of solar wind speed, fail to significantly improve transit time prediction. However, a correlation is found to exist between the late/early arrival of an ICME and the width of the preceding sheath region, suggesting that the error is a geometrical effect that can only be removed by a more accurate determination of a CME trajectory and expansion. The correlation between magnetic field intensity and speed of ejecta at 1 AU is also investigated. It is found to be weak in the body of the ICME, but strong in the sheath, if the upstream solar wind conditions are taken into account.

Key words. Solar physics, astronomy and astrophysics (flares and mass ejections) – Interplanetary physics (interplanetary magnetic fields; sources of the solar wind)

1 Introduction

Coronal mass ejections (CMEs) are known to be the major cause of severe geomagnetic disturbances, now often referred to as space weather (e.g. Daglis, 2001; etc.). In view of the possible deleterious effect of space weather on space- and ground-based technical systems (e.g. spacecraft charging, lowering of orbit, communication interruptions, flow of induced currents along transmission lines), making a prediction of the arrival time of a CME at 1 AU, and its properties at that time, is highly desirable. In principle, one would like

to be able to continually monitor the Sun using both full-disk imagers and coronagraphs (e.g. St. Cyr et al., 2000), so that an Earth-bound CME can be readily identified, and its velocity, trajectory and spatial extent estimated. At present such observations are carried out by instruments on the Solar and Heliospheric Observatory (SOHO) spacecraft, although estimating these parameters is fraught with difficulties.

Other information on the properties of CMEs comes from in situ magnetic field and plasma measurements in the interplanetary medium (especially at 1 AU), where they are usually referred to as Interplanetary CMEs (ICMEs). Combining observations at 1 AU with those of the Sun then permits a direct association to be made in many cases between a solar event and its interplanetary manifestation (but as will be discussed later, this becomes difficult at solar maximum when CMEs are very common). One can then build up a picture of how the arrival time and speed of an ICME at 1 AU is related to the velocity at the Sun, with the ultimate aim of developing a forecasting tool which uses solar observables to make predictions at 1 AU. This has been attempted by some workers (e.g. Gopalswamy et al., 2000, 2001a; Vršnak and Gopalawamy, 2002), and the details of these models will be discussed further in Sect. 2.

Since it is now clear that the transit time of a CME from the Sun to 1 AU is in the region of 1–5 days, advance forecasting is, in principle, feasible. However, there are problems with such forecasting models due to (a) the difficulty in estimating the velocity and trajectory of the CME at the Sun with single spacecraft observations, (b) analysing ICMEs using single-point in situ measurements and (c) understanding the forces that act on the ICME in the interplanetary medium.

CMEs with a trajectory close to the Sun-observer line appear to the observer as an expanding bright ring, or halo around the occulting disc of the coronagraph (Howard et al., 1982). The halo feature is in fact the CME expanding azimuthally with respect to the observer as it moves radially away from the Sun. (Events that originate on the front and back side of the Sun can often be differentiated by looking for activity close to the centre of the solar disc;

St. Cyr et al., 2000.) Tracking a CME feature (usually the bright leading edge) in consecutive coronagraph images allows for the speed of the CME to be estimated. However, this coronagraph-derived speed is the component of the CME speed in the plane of the sky (i.e. the plane perpendicular to the Sun-observer line). Thus, for any non-limb CME (such as a halo event), measurements of speed and direction will suffer to some degree from a “projection effect” (e.g. Gopalswamy et al., 2000). So tracking a halo gives the expansion speed of a CME rather than its radial speed away from the Sun, and the precise trajectory and velocity of the CME hence cannot be determined with any guaranteed accuracy.

In the heliosphere, ICMEs can be identified in magnetic field and plasma data by an enhanced magnetic field magnitude and sometimes a reduced proton temperature (both lasting for of the order of 0.5–1 day at 1 AU). Furthermore, approximately half the ICMEs show a smooth rotation in the magnetic field direction (referred to as “magnetic clouds”: Burlaga, 1988). ICMEs are clearly large three-dimensional structures that are undergoing continual expansion as they pass 1 AU. They are often preceded by a shock wave and compressed sheath region. On the basis of single spacecraft observations, further assumptions are needed to infer their 3-D structure, and in particular, which part of the ICME one is actually sampling.

ICME speeds at 1 AU range from 400 km/s up to in excess of 700 km/s, close to that of the ambient solar wind. This should be contrasted with estimated speeds at the Sun ranging from 100–2000 km/s. Clearly the interaction of ICMEs with the ambient solar wind leads to a net “equalisation” of the respective velocities (e.g. Gopalswamy et al., 2000), a process that can be attributed to a process analogous to aerodynamic drag (Cargill et al., 1995; Vršnak and Gopalswamy, 2002). However, difficulties in understanding this drag make prediction of the ICME speed at 1 AU difficult.

This paper will discuss the forecasting of ICME properties at 1 AU, and in particular, focus on possible causes for the systematic error in arrival time of around 15% that these models give. Section 2 reviews the existing models. Section 3 summarises the data used in our analysis, and examines model error and Sect. 4 addresses causes of the error (projection effects, ambient solar wind properties and ambiguities of observations at 1 AU).

2 A summary of current ICME forecasting models

The present generation of forecasting models all predict the transit time of a CME to 1 AU. This time (τ) is defined as being the time between the first observation of the CME by a coronagraph, and the arrival of the leading edge of the ICME at 1 AU. For example, the leading edge of a magnetic cloud event is simply defined as the onset of the smooth field rotation and proton temperature reduction. For non-cloud events, the identification is somewhat more difficult, and varies slightly between different ejecta. Signatures used included the onset of a reduced proton temperature or density,

the start of a linearly declining velocity profile and a reduced variance in the magnetic field. The sole input for the models is the earthward speed of the CME in the corona (U). A brief outline of each model follows.

2.1 Gopalswamy et al. (2000) model: constant acceleration or deceleration

As we noted in the Introduction, CMEs exhibit a much wider range of speeds at the Sun (100–2000 km/s: Hundhausen, 1999; St. Cyr et al., 2000) than at 1 AU (300–1000 km/s; Gopalswamy et al., 2001a). If one notes that the velocity of the solar wind ahead of and behind an ICME is in the range 350–600 km/s, ICMEs are, depending on their speed relative to the solar wind, either accelerated or decelerated towards the solar wind speed. Gopalswamy et al. (2000) assumed that the acceleration was constant between the Sun and 1 AU, so that the total effective interplanetary acceleration (a_1) undergone by an ICME is:

$$a_1 = \frac{V(1 \text{ AU}) - U}{\tau}, \quad (1)$$

where $V(1 \text{ AU})$ is the ICME speed at 1 AU. Assuming such a constant acceleration, the travel time of the CME is then given by the solution of the simple kinematic relation:

$$S = U\tau + \frac{1}{2}a_1\tau^2, \quad (2)$$

where S is the distance travelled (1 AU). We refer to this as the G2000 model.

2.2 Gopalswamy et al. (2001a) model: cessation of acceleration before 1 AU

Gopalswamy et al. (2001a) noted that the G2000 model could not account for the observation that CMEs with a slow initial speed ($U < 500$ km/s) have an approximately constant arrival time of 4.2 days. The G2000 model was thus modified by assuming that ICME acceleration ceased at a heliocentric distance of 0.76 AU for all CMEs, irrespective of their initial speed (0.76 AU was found to best fit the data). Thus, the total transit time to 1 AU is the sum of the travel time to 0.76 AU at constant acceleration, and the travel time from 0.76 AU to 1 AU at constant speed:

$$\tau = \frac{-U + \sqrt{U^2 + 2a_2d}}{a_2} + \frac{1 \text{ AU} - d}{\sqrt{U^2 + 2a_2d}}, \quad (3)$$

where a_2 is an effective interplanetary acceleration, that is now derived empirically from quadrature observations of CMEs (see Sect. 3.2), and d is the acceleration cessation distance (0.76 AU in the present case). We refer to this as the G2001 model.

2.3 Vršnak and Gopalswamy (2002) model: aerodynamic drag

Several forces are expected to act on ICMEs as they move from the Sun to the Earth. Gravity is usually neglected

beyond a fraction of an AU. Magnetic forces may act well beyond their usual pre-supposed location in the inner corona (e.g. Chen, 1996), and will be discussed later. However, the major cause of deceleration in the interplanetary medium is likely to be the interaction of the ICME with the ambient plasma. In reality, this will be a complex collection of processes involving shock waves, generation of turbulence, etc., but these are often parameterised as an aerodynamic drag force of the form $AC_D(V - W)|V - W|$, where V is the speed of the centre of mass of the ICME, W is the solar wind speed, C_D is a drag coefficient, typically a number of order unity (Chen, 1989, 1996; Cargill et al., 1995, 1996) and A is the cross section of the ICME.

Vršnak and Gopalswamy (2002) proposed a model for estimating the ICME transit time when the only force acting upon the ICME in interplanetary space is the aerodynamic drag. They assumed that the drag force was linearly proportional to the relative velocity. (They demonstrated that this leads to little difference from a model where the drag was proportional to the square of the relative velocity, and we have confirmed this independently for the cases shown in this paper.) The equation of motion of an ICME at some heliocentric distance R ($R = r/r_s$, where r_s is the solar radius) is then:

$$\frac{dV}{d\tau} = \alpha R^{-\beta}(V - W), \quad (4)$$

where α and β are constants that parameterise the drag as a function of distance, and are determined from a best fit to the data (see below). The solar wind speed is given by Sheeley et al. (1997):

$$W(R) = W_0 \sqrt{1 - e \frac{2.8 - R}{8.1}}, \quad (5)$$

where W_0 is the asymptotic solar wind speed. Writing this in terms of R gives:

$$\frac{dV}{dR} = r_s \alpha R^{-\beta} \left(1 - \frac{W}{V}\right). \quad (6)$$

Numerical integration from the low corona ($R = 10$, where it is assumed $V = U$) to 1 AU then gives $v(R)$, and hence τ . This is referred to as the VG2002 model.

3 Assessment of the three models

3.1 Solar and interplanetary data

We now compare these models with observations of CME transit times. The required observations are the CME speeds and onset times at the Sun obtained from coronagraph observations, and the arrival times and speeds at 1 AU from in situ solar wind magnetic field and plasma measurements. Our main focus is on the interval starting in November 1997, when the Advanced Composition Explorer (ACE) spacecraft made its first measurements of the solar wind, to April 2001. Coronal observations of CMEs

were made by the Large Angle Spectroscopic Coronagraph (LASCO: Brueckner et al., 1995) on the SOHO spacecraft. The onset time and speed of halo CMEs were taken from the LASCO CME catalogue (compiled by S. Yashiro, G. Michalek and N. Gopalswamy: see http://cdaw.gsfc.nasa.gov/CME_list/index.html). In situ plasma and magnetic field data from the SWEPAM (McComas et al., 1998) and MAG (Smith et al., 1998) instruments on board ACE were used to identify ICMEs at 1 AU.

We note here that the onset times from this catalogue should not be confused with the actual “onset” of the CME at the Sun. The “onset time” in the LASCO catalogue is defined as the time of CME appearance in the C2 coronagraph, which has an occulting disc of radius $2r_s$, so that the CME transit distance used in this study will be somewhat less than 1 AU. However, the error in the start time may be exaggerated for cases when the CME is directed earthwards. For halo CMEs the precise altitude of the “onset” measurement depends upon their true angular extent: an angular width of 40° (80°) will result in an altitude of $3.7r_s$ ($1.2r_s$). Using the average speed of the CMEs in this study (669 km/s), results in an error in the onset time of ~ 40 min and as we shall see, this is small compared to the average transit time error.

Connecting observations of CMEs at the Sun and ICMEs at 1 AU is not trivial. When multiple halo CMEs are seen (as occurs frequently at times of solar maximum), simple arguments about the association of ICMEs with CMEs should be avoided as not all front-side halo CMEs lead to a recognisable ICME signature at 1 AU. Furthermore, multiple CMEs originating from the same source region, or regions with a small angular separation (i.e. comparable to half the average CME width $\sim 36^\circ$), within a day of each other, could lead to significant interaction between different CMEs (Gopalswamy et al., 2001b). In order to focus in particular on the interplanetary forces acting on ICMEs, this study is restricted to cases where there is no ambiguity between solar and interplanetary observations. Hence, periods containing multiple halo CMEs were excluded.

To be confident that a CME and ICME are manifestations of the same ejection from the Sun (and are not subject to strong interaction with other ejecta), we require that an observation of a single halo CME (preferably with associated activity close to the centre of the solar disc) be followed 1 to 5 days later by a clear ICME signature in the magnetic and plasma data at 1 AU. However, as this study is based upon observations performed around Solar Maximum, such ideal situations are quite rare. Hence, the selection criteria must be relaxed if there are to be enough CME-ICME pairs to make comparison to models feasible. Thus, in general, multiple halo CMEs were considered to be non-interacting (and hence included in the study), if their 1 AU signatures were separated by at least a day. Using the ACE and SOHO data sets from November 1997 to April 2001, 35 CME-ICME pairs of reasonable confidence were identified. These events comprise the main data set used in this study, which is referred to as the Earth-Sun (E-S) line data.

Table 1. The five additional CME-ICME pairs.

ICME			CME			Transit time (days)
Date	UT	V (km/s)	Date	UT	U (km/s)	
28 Jan 1998	19:40	375	25 Jan 1988	15:22	693	4.18
12 Aug 2000	05:02	586	9 Aug 2000	16:34	702	2.52
13 Oct 2000	16:48	402	9 Oct 2000	23:46	798	3.71
29 Oct 2000	00:00	380	25 Oct 2000	08:24	770	3.65
28 Apr 2001	16:34	666	26 Apr 2001	12:29	1006	2.17

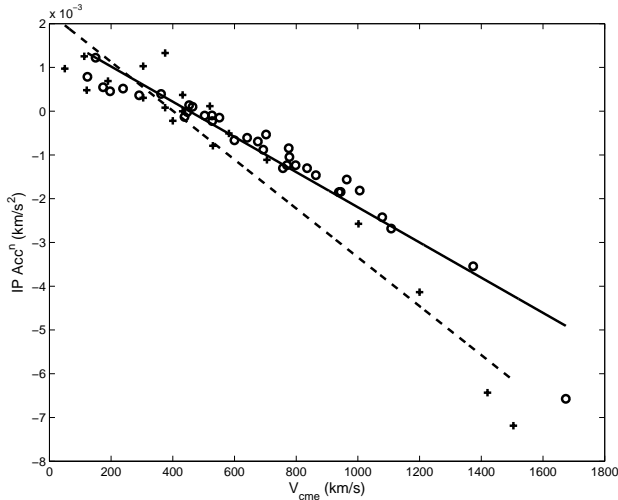


Fig. 1. The interplanetary acceleration as a function of the CME speed (U) at the Sun. The open circles correspond to the 35 CME – ICME pairs observed along the Earth-Sun line and the solid line shows the linear fit: $a_1(\text{km/s}^2) = -10^{-3}[0.0040U(\text{km/s}) - 1.8]$. The plus signs correspond to the 19 CME – ICME pairs observed in quadrature, and the dashed line shows the linear fit: $a_2(\text{km/s}^2) = -10^{-3}[0.0054U(\text{km/s}) - 2.2]$.

Gopalswamy et al. (2001a) published a list of 47 CME-ICME pairs using data from the WIND spacecraft and LASCO, 12 of which occurred before ACE became operational. A further 5 event pairs were excluded from this study as being multiple halos. Five events that do not appear in their list were used in this study. Thus, 30 CME-ICME pairs are common to both studies. In the interest of brevity, events common to both surveys are not listed here. Events 1–12 and 16 of Gopalswamy et al. (2001a) were not used due to lack of ACE data, while events 25, 30, 32 and 41 were not included due to insufficient confidence in the association. Table 1 lists the additional events in a similar format to Gopalswamy et al. (2001a).

A second data set used in this study consists of quadrature observations of CMEs (i.e. remote coronagraph observations made from the Earth-Sun line, and quadrature in situ measurements of ICMEs made over the limb of the Sun). Lindsay et al. (1999) compiled a list of such events using the Solar

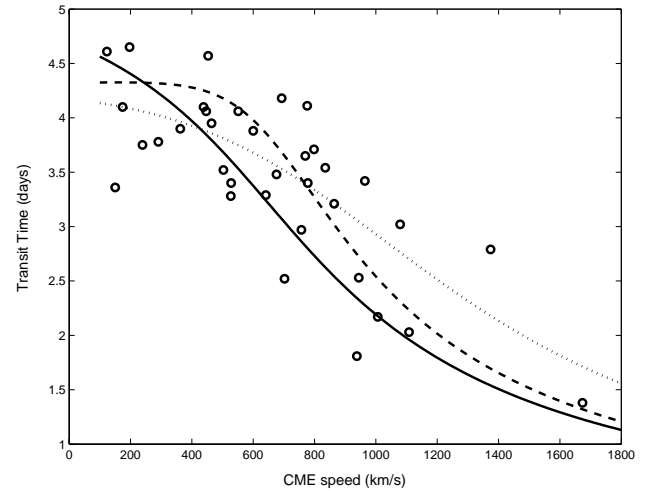


Fig. 2. The transit time of a CME to 1 AU as a function of the CME speed for the 35 E-S line events. The solid, dashed and dotted lines represent the transit time predicted by models G2000, G2001 and VG2002, respectively.

Maximum Mission (SMM) and Solwind coronagraphs, and the Helios 1 and Pioneer Venus Orbiter (PVO) in situ magnetic field and plasma measurements. Our study uses the slightly modified list of 19 events published by Gopalswamy et al. (2001a). The in situ observations of these ICMEs were made at heliocentric distances ranging from 0.63 to 0.92 AU.

3.2 Errors in the models

The circles in Fig. 1 show the effective interplanetary acceleration (a_1) undergone by the 35 E-S line CMEs as a function of their coronal speed (U). From the G2000 model, a linear fit to the data (solid line) is given by:

$$a_1(\text{km/s}^2) = -10^{-3} [0.0040U(\text{km/s}) - 1.8], \quad (7)$$

and we note that Gopalswamy et al. (2000) found a similar result for their list of E-S line CMEs:

$$a(\text{km/s}^2) = -10^{-3} [0.0035U(\text{km/s}) - 1.41]. \quad (8)$$

This empirically derived relation for a_1 as a function of U can then be used to predict the transit time of a CME to 1 AU,

Table 2. Comparison of models with the observations of the 35 E-S line CMEs.

Model	$\langle \Delta\tau \rangle$ (days)	$\langle \Delta\tau \rangle$ (days)	$\langle \Delta\tau \rangle / \tau$	$\langle \Delta V \rangle$ (km/s)	$\langle \Delta V \rangle / V$
G2000 - constant acceleration	0.51	-0.26	0.15	90.0	0.19
G2001 - acceleration cessation	0.46	0.10	0.15	100.8	0.20
VG2002 - aerodynamic drag	0.41	0.05	0.14	56.1	0.11

if constant acceleration is assumed. Figure 2 shows the observed transit time (circles) as a function of CME speed, with the solid line showing the transit time predicted by the G2000 model. The average error between the predicted and actual transit times ($\langle |\Delta\tau| \rangle$) is 0.51 days and the fractional error $\langle |\Delta\tau| \rangle / \tau = 0.15$. The distribution of $\Delta\tau$ is skewed ($\langle \Delta\tau \rangle = -0.26$), and hence, the G2000 model systematically overestimates CME transit times. Figure 3 shows the ICME speed (averaged over the duration of the event) for ejecta along the E-S line (circles) and the quadrature events (crosses) as a function of the CME speed at the Sun. For the G2000 model, the average error ($\langle \Delta V \rangle$) is 90.1 km/s and the percentage error ($\langle \Delta V \rangle / V$) is 0.19. The quality of the fit of the G2000 and G2001 models are discussed more fully in Gopalswamy (2002).

The crosses in Fig. 1 indicate the interplanetary acceleration for the 19 quadrature observations. The linear fit is given by:

$$a_2(\text{km/s}^2) = -10^{-3} [0.0054U(\text{km/s}) - 2.2] \quad (9)$$

(Gopalswamy et al., 2001) and is shown by the dashed line on Fig. 1. Assuming a constant acceleration of magnitude a_2 to 0.76 AU, and then a constant ICME speed to 1 AU, the G2001 model B then gives $\langle |\Delta\tau| \rangle = 0.46$ days, $\langle \Delta\tau \rangle = 0.10$, $\langle |\Delta\tau| \rangle / \tau = 0.15$, $\langle \Delta V \rangle = 108$ km/s and $\langle \Delta V \rangle / V = 0.2$ (dashed line on Figs. 2 and 3). Note that use of Eq. (9) in the G2000 model will lead to an increase in $\langle |\Delta\tau| \rangle$ due to longer travel times of faster CMEs.

Vršnak and Gopalswamy (2002) used aerodynamic drag coefficients of $\alpha = -0.002$ and $\beta = 1.5$, and a solar wind speed at 1 AU (W_o) of 400 km/s. In this study these three parameters were allowed to vary so as to minimise the difference between the predicted and actual 1 AU transit times ($\Delta\tau$). A simplex search method was used (Lagarias et al., 1998). We find that $\alpha = -0.0021$, $\beta = 1.34$ and $W_o = 438.1$ km/s gives the best fit. Using these parameters in the VG2002 model then gives $\langle |\Delta\tau| \rangle = 0.41$ days, $\langle \Delta\tau \rangle = 0.05$, $\langle |\Delta\tau| \rangle / \tau = 0.14$, $\langle \Delta V \rangle = 56$ km/s and $\langle \Delta V \rangle / V = 0.11$ (dotted line on Figs. 2 and 3).

The results for the three models are summarised in Table 2, which also shows the average and percentage errors in the velocity at 1 AU (ΔV : right-hand columns). It should be noted that despite the considerable difference in the assumptions in each of the models, the average error in the transit time is effectively the same for all three models. The VG2001 model appears to do somewhat better in the prediction of the ICME velocity at 1 AU. We also examined how the results

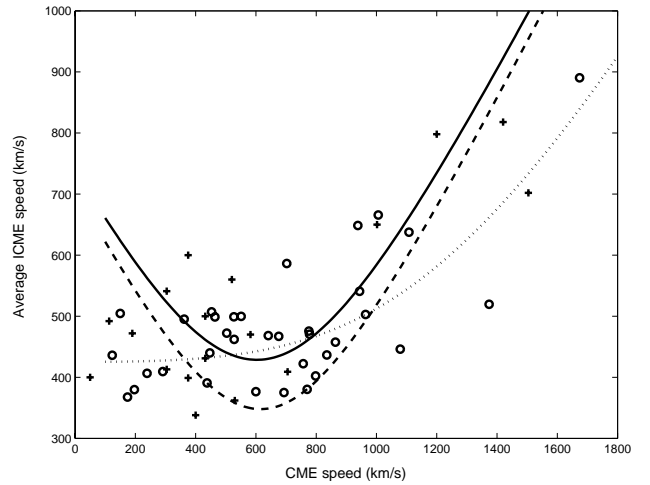


Fig. 3. The CME speed as a function of the average ICME speed at 1 AU for the 35 events observed along the Earth-Sun line (“o”s) and the 19 events observed in quadrature (“+”s). The solid, dashed and dotted lines represent the ICME speeds at 1 AU predicted by models G2000, G2001 and VG2002, respectively.

were altered by defining the transit time by the arrival of a shock front preceding an ICME. The best fit parameters of the models varied slightly to fit a decreased transit time, but the average error between the predicted and observed transit times remained approximately 11 h.

From Fig. 2 it is clear that the large range in τ (approximately 1.5 days) for CMEs with similar coronal speeds is responsible for the large value of $\langle |\Delta\tau| \rangle$ found for all 3 models. Hence, refining the existing models without incorporating further parameters is unlikely to achieve a significant increase in the accuracy of ICME arrival prediction. It is necessary to either reduce the error in the model input (the CME speed at the Sun), or to include further parameters, such as solar wind speed or precise CME trajectory. The relative importance of such factors is investigated in the following section.

4 Possible sources of error

Three possible factors influencing the accuracy of τ and U are investigated: (a) projection effects that may lead to an under-estimate of the CME speed at the Sun; (b) the assumption that the ambient solar wind conditions are the same for

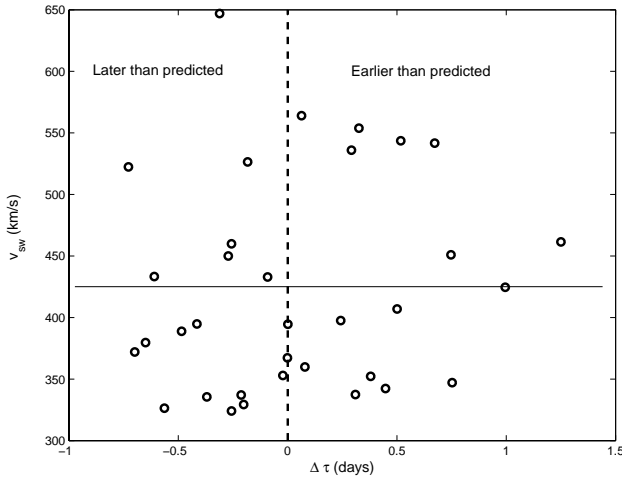


Fig. 4. The difference between the predicted and observed transit times to 1 AU ($\Delta\tau$) against solar wind speed upstream of the ICME. Positive (negative) values of $\Delta\tau$ correspond to ICMEs that arrive earlier (later) than predicted. The solid horizontal line shows the average upstream solar wind speed of 427 km/s. There does not appear to be any correlation between the late/early arrival of ICMEs and the upstream solar wind speed.

each CME and (c) the point of intersection of the spacecraft and the ICME, as inferred from observations of the sheath region.

4.1 CME speed at the Sun

When the location of the CME source on the solar surface is known (from X-ray or EUV observations), a simple geometric correction can be applied to the plane of sky speed to infer the radial speed if the CME width is known. (Of course, it needs to be stated that such corrections are subject to errors due to the fact that the X-ray activity can be located anywhere under the CME; e.g. Harrison, 1986.) Gopalswamy et al. (2001a) assumed an average CME width of 72° , but found the error between the predicted and observed transit times increased when the corrected speeds were used. It should be noted that the average width of 72° covers a wide range of values, thus the error introduced by assuming that all CMEs have the same angular width is greater than that introduced by the projection effect. A further difficulty with correcting for projection effects is the difficulty in relating the observed halo CME with matter actually moving earthwards. While simple cosine projections are commonly used, more sophisticated models may be needed to give the correct radial speeds (e.g. Zhao et al., 2002).

Bearing in mind these caveats, two methods of assessing the error introduced by the projection effect in predicting τ are investigated in this study. The first is to use a data set for which projection to both speed and transit time is absent: i.e. the quadrature observations of CME – ICME pairs. The effective interplanetary acceleration (a_2 : shown in Fig. 1) for these 19 events is given by Eq. (9) and is the effective ac-

celeration averaged to a distance of 0.76 AU (the average heliocentric distance at which the in situ measurements were made). Thus, at heliocentric distances greater or less than 0.76 AU, it is unsurprising that predictions of transit time based upon this parameter are highly inaccurate: for the 19 quadrature observations (made at a range of heliocentric distances from 0.63 to 0.92 AU) the average error in τ is 0.54 days for the G2000 model, and 0.55 for the G2001 model, in agreement with the estimates of Gopalswamy et al. (2001).

The VG2002 model does not use an effective total acceleration, but is based on the assumption that the deceleration of the ICME at any heliocentric distance is proportional to its speed relative to the ambient solar wind. Using best-fit parameters of $\alpha = -0.002$, $\beta = 1.48$ and $W_o = 524$ km/s obtained for this set of observations, the average error in τ is 0.46 days, comparable to the non-quadrature observations (0.41 days). The best-fit aerodynamic drag coefficients for the quadrature and E-S line observations are also similar, but the quadrature observations require a significantly higher solar wind speed (524 km/s compared to 438 km/s). It should be noted that due to the small number of events, the phase-space minima used to locate the best-fit parameters is quite broad (e.g. constraining W_o to a more reasonable 438 km/s still allows a fit to be achieved whereby the average error in τ is 0.52 days). For this reason we do not make any physical interpretation of the best-fit parameters.

As a second method for assessing the speed projection effect, we use the VG2002 model, but with the ICME speed at 1 AU speed as the sole input parameter, and integrate back to the Sun, and compare the time the CME was predicted to have left the Sun with the actual onset time there. This effectively removes the plane of sky projection error from the estimate of transit time. For the 35 E-S line events, this gave $< |\Delta\tau| > = 0.38$ days (compared to 0.41 days with the projection). Hence, the removal of the projection effect yields only a minor improvement (~ 0.03 days) in the prediction accuracy of the transit time. These two results, coupled with the findings of Gopalswamy et al. (2001a), lead us to conclude that projection effects are not the major cause of the error in the transit times.

4.2 Solar wind conditions

All the models discussed so far have assumed that the ambient solar wind conditions are the same for each ICME. Indeed the G2000 and G2001 models do not explicitly include an ambient solar wind speed (V_{sw}), but CMEs with $U > 406$ km/s are assumed to decelerate while those with $U < 406$ km/s are accelerated during their transit to 1 AU. The best-fit parameters of the VG2002 model use a solar wind speed of 438 km/s. However, the actual speed of the ambient solar wind in the ecliptic plane is known to vary from ~ 300 km/s to ~ 600 km/s (e.g. Phillips et al., 1995). This section assesses the error introduced into CME transit time prediction by the assumption of a constant solar wind speed at 1 AU.

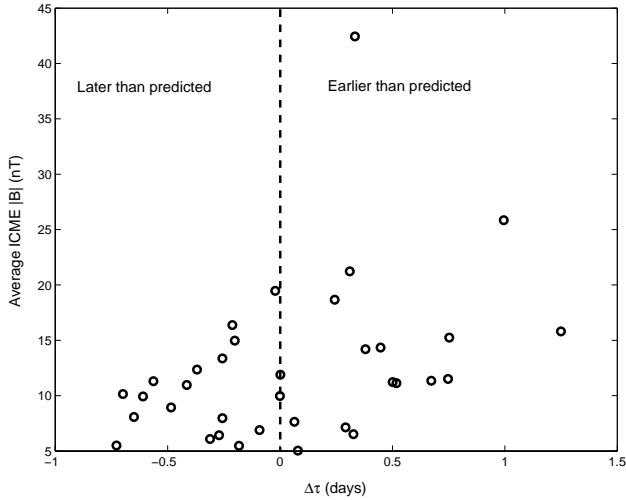


Fig. 5. The average magnetic field intensity of an ICME as a function of $\Delta\tau$ (predicted – actual τ). Late arriving ejecta have lower magnetic field intensities than early ones.

The ambient solar wind speed encountered by an ICME is defined as the average solar wind speed for 12 h upstream of the ICME-driven shock front, or upstream of the leading edge of the ICME for cases when a shock was not present. Different definitions of the ambient solar wind speed (e.g. 1 h to 1 day upstream averages) do not greatly affect our results. The solar wind speed (V_{sw}) experienced by the 35 E-S line ICMEs ranged from 324 km/s to 647 km/s, with an average of 427 km/s. For a CME with $U = 800$ km/s, an increase in solar wind speed from 324 to 647 km/s would decrease the value of τ predicted by the VG2002 model from 4.3 days to 2.5 days. Thus, the variation in V_{sw} is potentially significant.

Figure 4 shows the difference between the predicted and observed transit time to 1 AU ($\Delta\tau$ is negative for those ICMEs arriving later than predicted, positive for early) as a function of the solar wind speed. One would expect that higher solar wind speeds would lead to earlier arrivals, and lower speeds to later arrivals. In fact, there does not appear to be any correlation between $\Delta\tau$ and the solar wind speed. A similar lack of correlation was found for solar wind density and ram pressure (not shown). The net drag experienced by the ICME should depend on the ratio of the ICME to solar wind density, so that a denser solar wind would lead to a delayed arrival and vice versa. However, we note that in the VG2002 model, this density ratio is included in the best-fit parameters a and β .

Furthermore, using the observed values of V_{sw} as the parameter W_o in model C in fact increases $\langle |\Delta\tau| \rangle$ to approximately 0.6 days (compared to 0.41 days when all ICMEs are assumed to be embedded in an identical solar wind of speed 438 km/s).

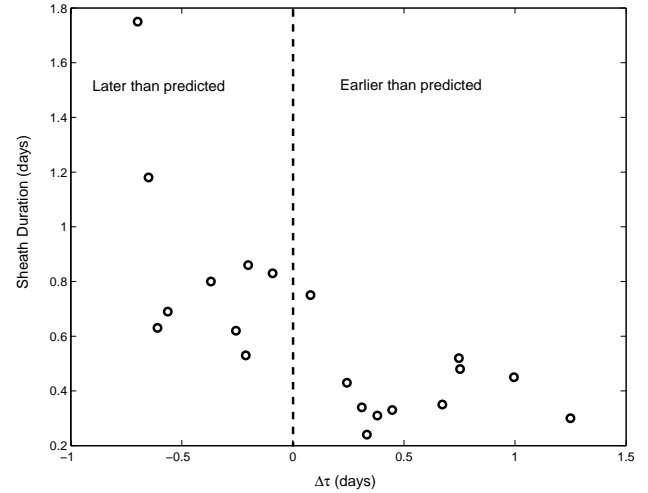


Fig. 6. Sheath region duration as a function of the difference between the predicted and actual transit time to 1 AU ($\Delta\tau$).

4.3 The role of the ICME magnetic field

The drag force will tend to equalise the speed of the ICME and solar wind, and clearly this is important in determining the observed speed of ICMEs at 1 AU. However, the flux rope nature of many ICMEs (e.g. magnetic clouds) implies that in some topologies there can be a significant outward Lorentz force (e.g. Chen, 1996). Thus, one should look for a correlation between early arrival and the average ICME magnetic field strength. In addition, as we shall discuss in Sect. 4.4, information about how $\Delta\tau$ depends on the field strength can yield clues to which part of an ICME one is encountering. In both cases, one would expect stronger fields to be associated with earlier arrivals. The result of such a study using the VG2002 model is shown in Fig. 5. There is a weak trend towards early arrival for stronger field strengths (the late ICMEs have an average magnetic field strength of 10.2 nT, while early ones have an average field of 14.8 nT). However, it should be noted that even using extremes of the distribution (i.e. the means of $|B|$ for ejecta with $\Delta\tau = \pm 0.3$ days), we could only discount the null hypothesis with an 80% confidence.

4.4 Properties of the ICME sheath region

Of the 35 E-S line events studied, 20 had an identifiable upstream shock front, and subsequent sheath region, preceding the main part of the ICME. Figure 6 shows the duration of the sheath region as a function of $\Delta\tau$ for these 20 events. The width of the sheath region can be estimated from the average plasma flow speed within the sheath. There is a clear trend for ICMEs with longer-duration sheath regions to arrive later than predicted: ICMEs arriving later than predicted (9 events) had an average sheath duration of 0.88 days and a sheath thickness of 3.4×10^7 km, whereas ICMEs arriving earlier than predicted (11 events) had an average sheath du-

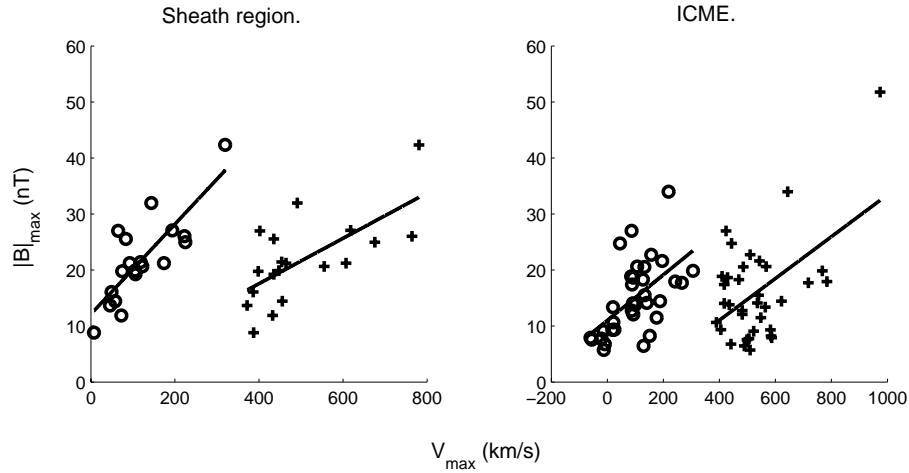


Fig. 7. The relationship between V_{\max} and $|\mathbf{B}|_{\max}$, $(V_{\max} - V_{sw})$ and $(|\mathbf{B}|_{\max})$ shown as “o”s (“+”s) for the sheath region and ICME body.

ration of 0.41 days and a thickness of 1.9×10^7 km. Thus, combining this with the results of the previous section, late arriving ICMEs have both thicker sheath regions and lower magnetic field intensities.

4.5 Predicting the magnetic field intensity at 1 AU

Prediction of the arrival time and velocity of an ICME at 1 AU is only the first step in space weather forecasting. The intensity of any triggered geomagnetic storm is dependent upon the ICME’s geo-effectiveness, which is determined by its velocity, and especially by the strength and duration of any southward IMF, both within the ICME itself and the preceding sheath region.

Previous studies have shown the existence of a linear relationship between maximum speed (V_{\max}) and maximum magnetic field intensity ($|\mathbf{B}|_{\max}$) of magnetic clouds (Gonzalez et al., 1998). Subsequently Owens and Cargill (2002) showed that such a relationship extended to all periods of the solar wind with a high magnetic field intensity (typically above 18 nT for a period of 3 h). Here we re-investigate this relation between magnetic field intensity and speed for the 35 E-S line ICMEs at 1 AU. For ICMEs that drive shocks, the relation is analysed for both the sheath region and the ICME itself, as defined in Sect. 2. The results are shown in Fig. 7, with crosses and circles representing the absolute speed and speed relative to the upstream solar wind of the ICME, respectively. Table 3 gives details of the linear best-fit parameters: the correlation is strong between the maximum speed relative to the solar wind and the maximum magnetic field intensity of the sheath region. However, we find a much weaker relationship between magnetic field intensity and speed within the body of the ICME, but note that two-thirds of the ICMEs used in this study had peak field intensities below the 18 nT threshold found by Owens and Cargill (2002) to give significant correlation.

Table 3. The relations between maximum field intensity and maximum speed, and maximum field intensity and maximum speed relative to the upstream solar wind are given for both the sheath region and ICME body for the 35 E-S line ICMEs. The linear best fit parameters (in the form $|\mathbf{B}| = mV + c$), χ^2 and linear correlation coefficient (r) are given.

		Linear Best Fit ($ \mathbf{B} = mV + c$)			
		m	c	χ^2	r
Sheath	$ \mathbf{B} - (V_{\max} - V_{sw})$	0.080	12.12	0.017	0.81
	$ \mathbf{B} - V_{\max}$	0.040	1.38	0.027	0.67
ICME	$ \mathbf{B} - (V_{\max} - V_{sw})$	0.041	10.99	0.036	0.56
	$ \mathbf{B} - V_{\max}$	0.037	-3.91	0.027	0.51

4.6 Interpretation

It is clear that little improvement in estimating ICME arrival time can be expected from efforts to model the effects discussed in Sect. 4.1 and 4.2. The lack of dependence on the projection angle suggests that either halo CMEs are structures that exhibit some sort of spherical symmetry, so that the velocity seen in the plane of the sky is approximately the same as that directed earthwards, or that if there is not exact spherical symmetry, the difference in the component of velocity directed Earthwards from the total velocity is small. Indeed recent results using LASCO data from Michalek et al. (2003) for an extensive sample of halo CMEs originating away from Sun-centre indicate that the difference between the plane of the sky and actual speeds may differ by only 20%.

In a complementary study, Gopalswamy et al. (2001a) attempted to reduce the projection effect in E-S line observations of halo CMEs by using the latitude and longitude of the source region, and assuming a CME average width of 72° .

They concluded that the discrepancy between the model and the observations increased when the CME speeds were corrected for possible plane-of-sky projection by using a simple geometry and an average cone angle for all CMEs. However, our null results suggest that projection is not the major cause of the observed spread in 1 AU transit times. Furthermore, the azimuthal expansion speed of a halo CME, as measured by a coronagraph at the L1 point, appears to be a good proxy for the radial speed of a CME along the E-S line, and hence, may be an adequate input for this class of models.

The lack of dependence on the ambient solar wind speed is surprising since it is clear that the relative motion between the ICME and solar wind is an important factor in determining the ICME speed, and the associated aerodynamic drag force will depend on the relative speed. It is unlikely that this is a result of single-point measurements of the solar wind. Solar wind structures usually extend over a significant fraction of a CME size.

The only quantity studied that showed a significant correlation with the error in the transit time was the thickness of the sheath ahead of the ICME, although there was also a weak correlation with the magnetic field strength. In fact, these results have mutual explanations, as shown in Fig. 8. The observed sheath thickness ahead of an ejecta is determined by both the physical properties of the ICME (especially its speed, since slower CMEs will have wider, but weaker sheaths) and the point of observation. One explanation focuses on the spatial properties characteristic of plasma sheaths associated with moving objects. The thickness of a sheath ahead of the main part of the ICME is known to increase with distance from the nose of a curved ICME (Russell and Mulligan, 2002); thus, a spacecraft intersecting an ICME away from the nose should see a wider sheath coupled with a longer apparent transit time than one flying through the middle. This is sketched in the left part of Fig. 8, where spacecraft A goes through the centre of the ICME, seeing a narrow sheath, while spacecraft B goes through the edge, and sees a broader sheath. For the same ICME, spacecraft A would report an earlier ICME arrival than spacecraft B, consistent with the tendency for late arrivals to be associated with a thicker sheath. This scenario can also account for the trends in the ICME magnetic field intensity. The magnetic field strength within a magnetic cloud falls off with distance away from the axis, where the axis is here defined as being along the direction of the ICME toroidal field (see Fig. 8). Thus, a late-arriving event would also see a reduced magnetic field intensity as the spacecraft passed through the edge of the ICME. Thus, we believe that the spread in τ could be due to a geometric effect.

A second possible explanation of the results in Sects. 4.3 and 4.4 arises from the result of recent numerical simulations (e.g. Vandas et al., 1995; Cargill et al., 2000), which indicate that the degree of deformation of the cross-sectional shape of an ICME by the solar wind depends upon the magnetic field intensity and topology within the ICME. This is illustrated in the right-hand part of Fig. 8, where an ICME with a weak magnetic field has undergone additional lateral expansion.

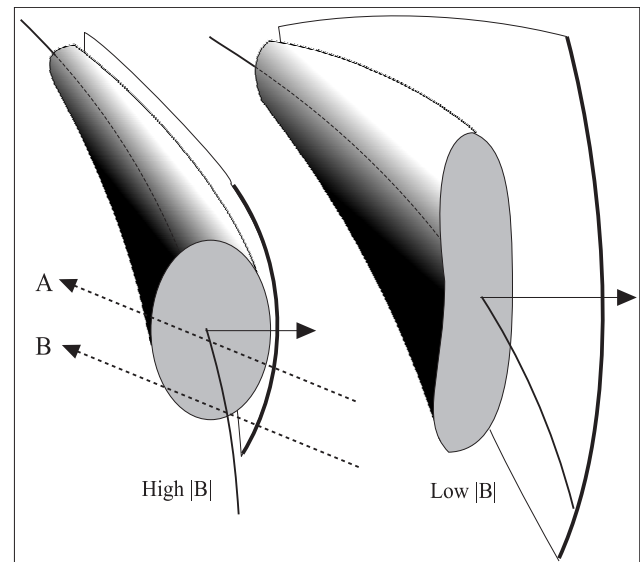


Fig. 8. A representation of possible ICME cross sections at 1 AU for high $|B|$ and low $|B|$ events. In the former case the string field leads to the ICME maintaining an approximately circular cross section, while for a weaker field, the ICME becomes elongated in the vertical direction in this sketch. The arrow denotes the direction of ICME motion, the curved line ahead of the ICME corresponds to a possible bow shock location and the solid line coming out of the body of the CME corresponds to a schematic axis of the ICME. Two possible spacecraft crossings are shown for the high $|B|$ picture: A passing close to the central axis, and B clipping the outer edge of the ICME.

sion. This lateral expansion will lead to an increase in the aerodynamic drag force (Cargill et al., 1995, 2000), and so a later arrival time. The wider, slower moving ICME will also have a thicker sheath region.

4.7 Discussion

We have examined models for the prediction of ICME arrival time at 1 AU that use as input the CME speed at the Sun. The models show a surprising similarity in the average error in ICME arrival time. An exploration of possible sources of error leads to the conclusion that the primary cause of error is most likely a geometrical effect, as opposed to being due to projection effects at the Sun, or the use of simplified solar wind parameters. The geometrical effects can arise for two reasons. First, from a single in situ observation of an ICME, one does not know which part of the event one is sampling. An ICME is a curved three-dimensional structure, and the measured arrival time will depend on which part of the ICME is being sampled. Second, ICMEs become deformed in the interplanetary medium, with an elongation taking place in a direction perpendicular to the principle direction of motion. In both cases, late detection of the ICME will be associated with weaker magnetic fields, as indeed we find. To resolve this issue needs (as a minimum) a more accurate determination of the direction of ICME propagation such as could be provided by STEREO measurements.

Our results appear to suggest that CME velocities at the Sun measured in the plane of the sky are adequate for ICME prediction, provided, of course, one can associate these with a halo event, and that a simple solar wind model is adequate. However, one can expect STEREO observations to give a better determination of the velocity vector of the CME at the Sun, and it is easy with an L1 monitor to use real-time ambient solar wind data. But for forecasting the ICME arrival time, the L1 solar wind parameters are not essential (of course, they are essential for understanding what effect the ICME has on the magnetosphere and ionosphere).

An important new measurement would be enhanced precision in the direction of ICME propagation. This would enable one to not only improve the ICME arrival time, as we have noted in this paper, but also to make a prediction about its geo-effectiveness. An ICME that strikes a “glancing blow” at the Earth will not only lead to a weaker IMF (see Sect. 4.6), but also any interval of southward IMF will be shorter (Cargill et al., 1994). The forthcoming STEREO mission provides an excellent opportunity to see if realistic estimates of ICME propagation can really lead to significant improvements in space weather forecasting.

Finally, we note that the perennial difficulty with predicting the magnetic field strength of an ICME remains unresolved. Although our earlier work showed good correlations between the solar wind velocity and maximum field strength for events with a maximum field > 18 nT, the correlation is actually weaker when one restricts the analysis to ICMEs. This is due to a dominance of events with lower magnetic fields, a possible consequence of “off-axis” ICME crossings (i.e. path B in Fig. 8). However, the correlation between speed and magnetic field intensity is significant relative to the solar wind speed in the sheath region. This relation could be the result of draping of the solar wind magnetic field in front of the faster moving ICME. Thus, though prediction of solar wind speed at 1 AU may not be required to predict the arrival time of ICMEs, it is needed to forecast the magnetic properties of the sheath region.

Acknowledgements. We acknowledge support from PPARC and QuinetiQ. We have benefited from the availability of ACE data at NSSDC, in particular the MAG (P.I. N. Ness) and SWEPAM (P.I. D. McComas) instruments. The CME catalogue is generated and maintained by NASA and The Catholic University of America in cooperation with the Naval Research Laboratory. SOHO is a project of international cooperation between ESA and NASA. We would also like to thank Adam Rees for useful discussions.

The Editor in Chief thanks two referees for their help in evaluating this paper.

References

- Brueckner, G. E., Howard, R. A., Koomen, M. J., Korendyke, C. M., Michels, D. J., Socker, D. G., Dere, K. P., Lamy, P. L., Llebaria, A., Bout, M. V., Schwenn, R., Simnett, G. M., Bedford, D. K., and Eyles, C. J.: The large angle spectroscopic coronagraph (LASCO), *Sol. Phys.*, 162, 357, 1995.
- Burlaga, L. F.: Magnetic clouds: Constant alpha force-free configurations, *J. Geophys. Res.*, 93, 7217, 1988.
- Cargill, P. J., Chen, J., Spicer, D. S., and Zalesak, S. T.: The deformation of flux tubes in the solar wind with applications to the structure of magnetic clouds and CMEs, *Proc. of the Third SOHO Workshop*, 291, 1994.
- Cargill, P. J., Chen, J., Spicer, D. S., and Zalesak, S. T.: Geometry of interplanetary magnetic clouds, *Geophys. Res. Lett.*, 22, 647, 1995.
- Cargill, P. J., Chen, J., Spicer, D. S., and Zalesak, S. T.: MHD simulations of the motion of magnetic flux tubes through a magnetized plasma, *J. Geophys. Res.*, 101, 4855, 1996.
- Cargill, P. J., Schmidt, J., Spicer, D. S., and Zalesak, S. T.: The magnetic structure of over expanding CMEs, *J. Geophys. Res.*, 105, 7509, 2000.
- Chen, J.: Effects of toroidal forces in current loops embedded in a background plasma, *Astrophys. J.*, 338, 453, 1989.
- Chen, J.: Theory of prominence eruption and propagation: interplanetary consequences, *J. Geophys. Res.*, 101, 27 499, 1996.
- Daglis, I. A.: Space storms, ring current and space-atmosphere coupling, *NATO ASI Space Storms and Space Weather Hazards*, Kluwer Publishers, 2001.
- Gonzalez, W. D., Clua De Gonzalez, A. L., Dal Lago, A., Tsurutani, B. T., Arballo, J. K., Lakhina, G. S., Buti, B., and Ho, G. M.: Magnetic cloud field intensities and solar wind velocities, *Geophys. Res. Lett.*, 25, 963, 1998.
- Gopalswamy, N.: Relation between CMEs and ICMEs, in: “Solar-terrestrial Magnetic Activity and Space Environment”, *COSPAR Colloquia Series*, 14, edited by Wang, H. N. and Xu, R. L., p. 157, 2002.
- Gopalswamy, N., Lara, A., Lepping, R. P., Kaiser, M. L., Berdichevsky, D., and St. Cyr, O. C.: Interplanetary acceleration of coronal mass ejections, *Geophys. Res. Lett.*, 27, 145, 2000.
- Gopalswamy, N., Lara, A., Yashiro, S., Kaiser, M. L., and Howard, R. A.: Predicting the 1-AU arrival times of coronal mass ejections, *J. Geophys. Res.*, 106, 29 207, 2001a.
- Gopalswamy, N., Yashiro, S., Kaiser, M. L., Howard, R. A., and Bougeret, J.-L.: Radio signatures of coronal mass ejection interaction: Coronal mass ejection cannibalism?, *Astrophys. J.*, L91, 548, 2001b.
- Harrison, R. A.: Solar coronal mass ejections and flares, *Astron. Astrophys.*, 162, 283, 1986.
- Howard, R. A., Michels, D. J., Sheely, N. R., and Koomen, M. J.: The observation of a coronal transient directed at Earth, *Astrophys. J. Lett.*, 263, 101, 1982.
- Hundhausen, A. J.: Coronal mass ejections, in: *The many faces of the Sun*, edited by Strong, K. T., Springer Press, p. 143, 1999.
- Lagarias, J. C., Reeds, J. A., Wright, M. H., and Wright, P. E.: Convergence Properties of the Nelder-Mead Simplex Method in Low Dimensions, *SIAM Journal of Optimization*, 9, Number 1, 112, 1998.
- Lindsay, G. M., Luhman, J. G., Russell, C. M., and Gosling J. T.: Relationships between coronal mass ejection speeds from coronagraph images and interplanetary characteristics of associated interplanetary coronal mass ejections, *J. Geophys. Res.*, 104, 12 515, 1999.
- McComas, D. J., Bame, S. J., Barker, S. J., Feldman, W. C., Phillips, J. L., Riley, P., and Griffee, J. W.: Solar wind electron proton alpha monitor (SWEPAM) for the Advanced Composition Explorer, *Space Sci. Rev.*, 86, 563, 1998.
- Michalek, G., Gopalswamy, N., and Yashiro, S.: A new method for estimating widths, velocities and source location of halo coronal

- mass ejections, *Astrophys. J.*, 584, 472, 2003.
- Owens, M. J. and Cargill, P. J.: Correlation of magnetic field intensities and solar wind speeds of events observed by ACE, *J. Geophys. Res.*, 107, 1050, 2002.
- Phillips, J. L., Bame, S. J., Barnes, A., Barraclough, B. L., Feldman, W. C., Goldstein, B. E., Gosling, J. T., Hoogeveen, G. W., McComas, D. J., Neugebauer, M., and Suess, S. T.: Ulysses solar wind plasma observations from pole to pole, *Geophys. Res. Lett.*, 22, 3301, 1995.
- Russell, C. T. and Mulligan, T.: On the magnetosheath thicknesses of interplanetary coronal mass ejections, *Planetary and Space Sci.*, 50, 527, 2002.
- St. Cyr, O. C., Howard, R. A., Sheely, Jr., N. R., Plunkett, S. P., Michels, D. J., Paswaters, S. E., Koomen, M. J., Simnett, G. M., Thompson, B. J., Gurman, J. B., Schwenn, R., Webb, D. F., Hildner, E., and Lamy, P. L.: Properties of coronal mass ejections: SOHO LASCO observations from January 1996 to June 1998, *J. Geophys. Res.*, 105, 18 169, 2000.
- Sheeley, N. R., Jr., Wang, Y. M., Hawley, S. H., Brueckner, G. E., Dere, K. P., Howard, R. A., Koomen, M. J., Korendyke, C. M., Michels, D. J., Paswaters, S. E., Socker, D. G., St. Cyr, O. C., Wang, D., Lamy, P. L., Llebaria, A., Schwenn, R., Simnett, G. H., Plunkett, S. and Biesecker, D. A.: Measurements of the flow speed in the corona between 2 and 30 r_s , *Astrophys. J.*, 484, 472, 1997.
- Smith, C. W., L'Heureux, J., Ness, N. F., Acuna, M. H., Burlaga, L. F., and Scheifele, J.: The ACE magnetic fields experiment, *Space Sci. Rev.*, 86, 613, 1998.
- Vandas, M., Fischer, S., Dryer, M., Smith, Z., and Detman, T.: Simulation of magnetic cloud propagation in the inner heliosphere in two-dimensions: 1. loop perpendicular to the ecliptic plane, *J. Geophys. Res.*, 100, 12 285, 1995.
- Vršnak, B. and Gopalswamy, N.: Influence of aerodynamic drag on the motion of interplanetary ejecta, *J. Geophys. Res.*, 107, 10.1029/2001/JA000120, 2002.
- Zhao, X. P., Plunkett, S. P., and Liu, W.: Determination of geometrical and kinematical properties of halo coronal mass ejections using the cone model, *J. Geophys. Res.*, 10.1029/2001JA009143, 2002.